



OPEN

Molecular insights and antibody response to Dr20/22 in dogs naturally infected with *Dirofilaria repens*

Mateusz Pękacz¹, Katarzyna Basałaj², Daniel Młocicki³, Maciej Kamaszewski⁴, Elena Carretón⁵, Rodrigo Morchón⁶, Marcin Wiśniewski^{1,8} & Anna Zawistowska-Deniziak^{7,8}✉

Subcutaneous dirofilariasis, caused by the parasitic nematode *Dirofilaria repens*, is a growing concern in Europe, affecting both dogs and humans. This study focused on *D. repens* Dr20/22, a protein encoded by an *alt* (abundant larval transcript) gene family. While well-documented in L3 larvae of other filariae species, this gene family had not been explored in dirofilariasis. The research involved cloning Dr20/22 cDNA, molecular characterization, and evaluating its potential application in the diagnosis of dirofilariasis. Although Real-Time analysis revealed mRNA expression in both adult worms and microfilariae, the native protein remained undetected in lysates from both developmental stages. This suggests the protein's specificity for L3 larvae and may be related to a process called SLTS (spliced leader trans-splicing), contributing to stage-specific gene expression. The specificity of the antigen for invasive larvae positions it as a promising early marker for dirofilariasis. However, ELISA tests using sera from infected and uninfected dogs indicated limited diagnostic utility. While further research is required, our findings contribute to a deeper understanding of the molecular and immunological aspects of host-parasite interactions and could offer insights into the parasite's strategies for evading the immune system.

Subcutaneous dirofilariasis is a vector-borne disease caused by a parasitic nematode *Dirofilaria repens*. Owing to climate changes and anthropogenic activities, dirofilariasis has expanded its distribution across nearly all European countries¹. Consequently, it has emerged as one of the most rapidly spreading parasitoses in the Old World. While the primary hosts of the disease are carnivores, notably dogs, it exhibits considerable zoonotic potential, thereby constituting a significant concern in both medical and veterinary fields. However, due to the predominantly asymptomatic or mildly symptomatic nature of *D. repens* infections², this zoonosis has often been overlooked, particularly when compared to other filariasis such as pulmonary dirofilariasis or lymphatic filariasis. As a result, research efforts aimed at mitigating invasions, such as early infection detection or development of potential vaccines, have been substantially impeded, given the limited understanding of the parasite's biology and the molecular interactions it established with the hosts.

Throughout the protracted co-evolution between hosts and parasites, helminths have evolved diverse strategies to evade host immune responses at various stages of their life cycle^{3–6}. Notably, the filariae L3 larvae adeptly evade and down-modulate the host's immune system within the cutaneous tissues, playing a pivotal role in both the parasite's establishment and the development of host immunity⁷. These immunomodulatory properties are primarily attributed to the surface and secreted antigens displayed by the larvae. As the initial molecules that engage the definitive host's immune system, these antigens hold promise as potential early markers of infection.

¹Division of Parasitology, Department of Preclinical Sciences, Institute of Veterinary Medicine, Warsaw University of Life Sciences-SGGW, 02-786 Warsaw, Poland. ²Museum and Institute of Zoology, Polish Academy of Sciences, 00-818 Warsaw, Poland. ³Department of General Biology and Parasitology, Medical University of Warsaw, 02-004 Warsaw, Poland. ⁴Department of Ichthyology and Biotechnology in Aquaculture, Institute of Animal Sciences, Warsaw University of Life Sciences-SGGW, 02-786 Warsaw, Poland. ⁵Internal Medicine, Faculty of Veterinary Medicine, University of Las Palmas de Gran Canaria, Campus Arucas, Arucas, 35413 Las Palmas, Spain. ⁶Zoonotic Diseases and One Health Group, Faculty of Pharmacy, University of Salamanca, Campus Miguel Unamuno, 37007 Salamanca, Spain. ⁷Department of Immunology, Institute of Functional Biology and Ecology, Faculty of Biology, University of Warsaw, 02-095 Warsaw, Poland. ⁸These authors contributed equally: Marcin Wiśniewski and Anna Zawistowska-Deniziak. ✉email: a.zawistowska-deniziak@uw.edu.pl

Moreover, the presence of antibodies against L3 larvae is hypothesized to suppress larval development and correlate with resistance to new infections^{8,9}. However, despite the critical roles, the specific molecules underlying immune modulation in *D. repens* remain elusive. Thus, an in-depth investigation into stage-specific antigens, along with their molecular and immunological characterization, may offer novel insights into the development of prospective vaccines or diagnostic tools.

In light of this, the present study focused on a singular L3-specific *D. repens* 20/22 kDa protein (GenBank: QHR84804.1) known as Dr20/22, which was produced in recombinant form. Dr20/22 is encoded by a gene belonging to the *alt* (abundant larval transcript) family, a group well documented in numerous filarial nematodes including *Brugia malayi*^{10,11}, *Onchocerca volvulus*¹², *Acanthocheilonema viteae*¹³, *Wuchereria bancrofti*¹⁴ and *Dirofilaria immitis*^{15,16}. The ALTs being abundantly expressed in invasive larvae and mammals are devoid of known homologues. Given this, the proteins represent highly attractive vaccine candidates for filarial infections. While the precise biological function of these antigens remains obscure, extensive research has been conducted to explore their prophylactic potential, particularly in human lymphatic filariasis caused by *B. malayi* and *W. bancrofti*^{11,14,17–24}. Intriguingly, however, no investigations have yet delved into this antigen in the context of subcutaneous dirofilariasis. Thus, the *D. repens* homologue of ALT might hold central importance in the invasion process, and its comprehensive molecular and immunological characterization could represent a critical milestone in advancing our understanding of the intricate host-parasite interactions.

This study entailed the cloning of cDNA encoding the *D. repens* homologue of ALT (Dr20/22), followed by its meticulous molecular characterization. Subsequently, the recombinant antigen was evaluated for its potential application as an early diagnostic marker for subcutaneous dirofilariasis and used to discern antibody responses in dogs naturally infected with *D. repens* in comparison to non-infected individuals.

Results

Cloning and characterization of cDNA and gDNA of the Dr20/22 gene in *D. repens*

The cDNA cloning of the *dr20/22* gene yielded a 417 bp product. The complete coding sequence of the *D. repens alt* gene homologue in its adult stage was submitted to GenBank under accession number MN706526.1. No *D. repens*-specific SL sequence was found in either the adult stage or the microfilariae stage cDNA. Additionally, the gDNA cloning of almost the entire gene (from the start codon to the stop codon) resulted in a 1048 bp product (Supplementary Fig. 1).

Comparative analysis of nucleotide and amino acid sequences of ALT cDNAs from related filariae reveals phylogenetic relationships and structural characteristics of Dr20/22 protein

Comparison of nucleotide sequences of ALT cDNAs from related filariae using Blast showed 82.12% identity to *D. immitis* (U29459.1), 76.19% to *Loa loa* (XM_003148107), 60.92% to *O. volvulus* (U29576.1), 78.52% to *A. viteae* (U47545.2), 77.29% to *W. bancrofti* (AF285860.1), and 72.98% to *B. malayi* (U84723.1). A comparison of cDNA and gDNA encoding Dr20/22 revealed that the gene consists of 4 exons (1–78 bp; 296–422 bp; 665–755 bp; 928–1048 bp) and 3 introns (Supplementary Fig. 1).

Comparison of amino acid sequences showed 75.69% (MCP9263779.1) and 72.85% (AAC47031.1) identity to *D. immitis*, 55.48% to *A. viteae* (AAB03902.2), 46.81% to *O. volvulus* (AAA84910.1), 64.10% to *L. loa* (XP_003148155.1), 56.62% to *W. bancrofti* (EJW81953.1), and 53.68% to *B. malayi* (AAB41884.1).

Analysis of the putative amino acid sequence revealed the presence of a 21 amino acid signal peptide, followed by a protein with a theoretical molecular mass of 13.82 kDa and pI 4.93. NetOGlyc and NetNGlyc biotools determined six potential O-glycosylation sites (in positions 27, 29, 33, 36, 53, 60) and no N-glycosylation sites. NetPhos revealed 18 potential sites of phosphorylation: serine (23, 27, 29, 33, 36, 67, 97, 107, 118, 125, 128), threonine (53, 60), tyrosine (37, 41, 58, 81, 126). InterProScan identified a Chromadorea ALT domain (IPR008451) in position 62–135 characteristic of a vast family of filariae. The Phyre² program constructed the most probable 3D structure based on bee-venom phospholipase A2 from *Apis mellifera* (PMID: 2274788). However, only 28% of the protein could be modeled, and the confidence level of this model was estimated at just 3.8%.

Real-time PCR analysis of *D. repens alt* gene expression

Gene expression analysis showed 3.32 times higher expression levels of the *D. repens alt* gene in the adult stage than in microfilariae (Fig. 1).

Expression and characterization of Dr20/22 recombinant protein

SDS-PAGE and Western blot analyses displayed the purified protein as a double band within the 20–22 kDa range (Fig. 2). Glycoprotein staining did not indicate the presence of any glycan residues (Fig. 3). Interestingly, when the gel was overloaded with the protein, smaller fragments of the protein were detected, implying a propensity of the protein to undergo collapse. This observation was further confirmed in subsequent Western blot analyses using frozen protein.

PLA₂ assay has shown no activity of the rDr20/22

As PLA₂ activity was not detected, we conducted tests to explore the protein stability and the potential impact of freezing on antigen activity. Both fresh protein (used immediately after purification) and protein subjected to a freeze–thaw cycle were examined. The rationale behind this testing approach was to ensure that if the protein did possess PLA₂ activity, it could be assessed for any potential loss or changes in activity resulting from the freezing process.

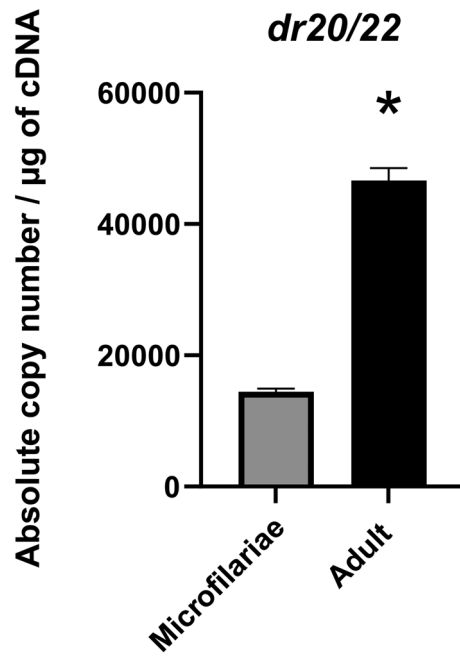


Figure 1. Analysis of the expression levels of *dr20/22* in microfilariae and the adult stage of *D. repens*. The result shows the number of gene copies per μg of cDNA. The bars show mean \pm SEM. The statistically significant differences between examined groups are marked with asterisks: * $p < 0.05$.

Lack of Dr20/22 detection in *D. repens* lysates from adult and microfilariae stages

The Western blot analysis confirmed the presence of antibodies targeting the recombinant Dr20/22 epitopes in the anti-Dr20/22 serum, while no specific antibodies were detected in the serum of non-immunized mice. It was previously mentioned that the freeze–thaw cycle resulted in the observation of smaller protein fragments (Fig. 4).

Native Dr20/22 was not detected in any of the tested *D. repens* lysates, including adult female worm, E/S fraction (data not shown), and microfilariae (data not shown). Some unintended bands were detected in each condition (1b, 2b, 3b) as a result of the non-specific binding of anti-mouse IgG with residual dog IgG present in the worm lysate (Fig. 4). However, specific localization of the protein in cross-sections of the adult female worm (Fig. 5) was not achieved. The anti-Dr20/22 serum showed a strong immunolabeling almost throughout the entire histological section, while a weak immunolabeling was also observed with the serum from non-immunized mice, suggesting the possibility of cross-reactions (Fig. 6).

Recognition of rDr20/22 by antibodies in sera from naturally infected dogs with *D. repens*

Western blot analysis revealed the presence of specific IgG antibodies against rDr20/22 in sera from dogs infected with *D. repens*, while no such antibodies were detected in dogs infected with *D. immitis* (Fig. 7).

ELISA with rDr20/22 reveals IgG response in both infected and negative groups

ELISA, utilizing adult somatic antigen (DrSA) facilitated the classification of dogs without active microfilaremia into amicrofilaremic (Mf⁻; N = 297) and uninfected (Neg; N = 379). Interestingly, within the microfilaremic group, several low responders were identified, showing antibody levels comparable to those in non-infected dogs (Fig. 8). This step was critical in further examination of the diagnostic potential of rDr20/22. All sera utilized in the experiment were from leftover blood samples obtained from both pet dogs and shelter dogs. Due to the lack of complete medical histories, we were unaware of any past infections with *Dirofilaria* or other parasites, as well as their current clinical status. By comparing the results to DrSA, we could more accurately assess the usefulness of the individual antigen.

Subsequently, we explored the IgM class in the dogs based on this classification, yet found no significant differences between the infected and non-infected groups (Fig. 9). As a result, we decided to exclude the IgM class from further investigations.

When tested the same panel of sera, rDr20/22 demonstrated elevated IgG levels in both infected groups; however, a notable proportion of uninfected dogs also exhibited heightened antibody levels.

Moreover, cross-reactivity in IgG was observed between dogs infected with *D. repens* and *D. immitis*, using crude antigens from adult worms of both species (DrSA/DiSA), as well as rDr20/22 (Fig. 10).

Discussion

In the present study, we successfully cloned cDNA and gDNA encoding the *D. repens* homologue of ALT, which we named Dr20/22. The predicted molecular weight was significantly lower than the actual size observed on the gel, similar to its orthologs in other filariae (15.1–15.8 kDa)^{12,13}. The observed double band on the gel may

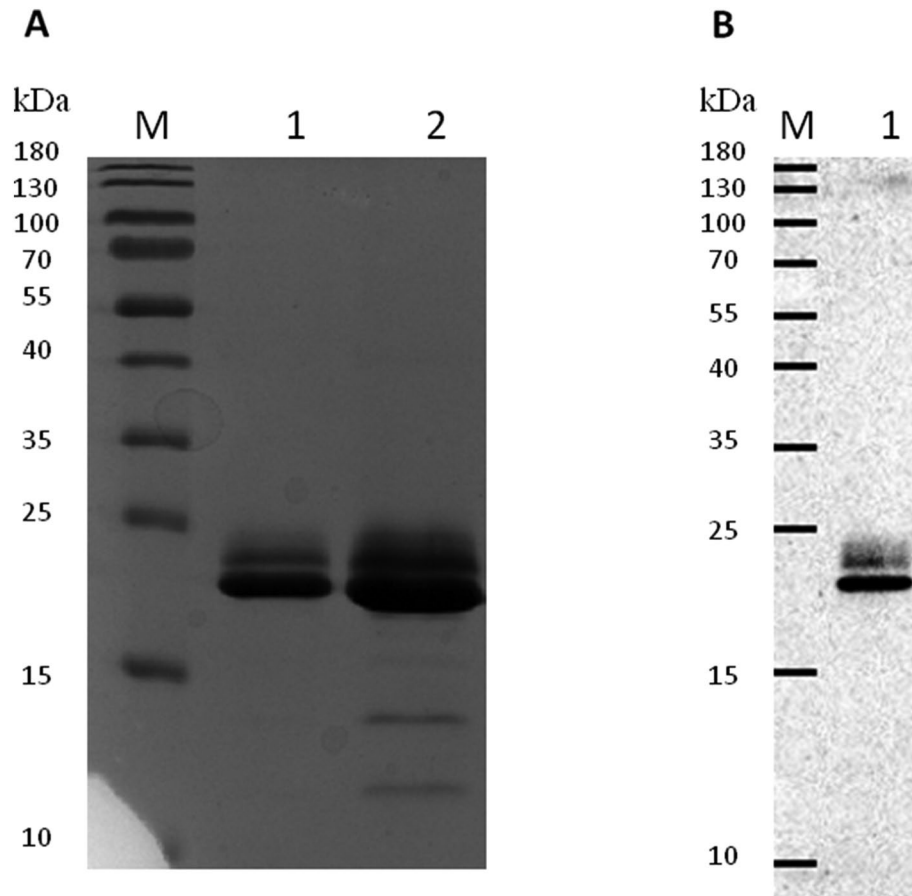


Figure 2. SDS PAGE (A) and Western blot (B) analysis of purified rDr20/22. The Western blot analysis employed the Anti-polyHistidine-Peroxidase antibody. The cropped gel and blot are used in the figure. Lane M—molecular weight marker (PageRuler Prestained Protein Ladder, 10 to 180 kDa, Thermo Scientific); lane 1A—5 μ g of the rDr20/22; lane 2A—15 μ g of the rDr20/22; lane 1B—0.25 μ g of the rDr20/22. Original gel and blot are presented in Supplementary Fig. 3.

result from posttranslational modifications, such as glycosylation and phosphorylation. A double band was also observed for *Brugia* ALT obtained in *Pichia pastoris* due to the glycosylation process¹⁷. Despite the presence of potential O-glycosylation sites, glycan residues were not confirmed by PAS staining in our study. Computational analyses predicted 18 phosphorylation sites for Dr20/22, with phosphorylation events potentially adding almost 1.5 kDa²⁵, which may explain the upper band. Genomic cloning revealed that the *dr20/22* gene consists of 4 exons and 3 introns (Supplementary Fig. 1), consistent with data from research on *B. malayi alt* genes²⁶. In most species, there are at least two transcription variants (*alt-1* and *alt-2*). Each variant has been identified as high stage-specific protein and is among the most abundant proteins in L3 larvae of several filariae species^{10–16}.

In our study, we demonstrated that the expression level of *dr20/22* mRNAs was approximately three times higher in the adult stage compared to microfilariae. However, surprisingly, we did not detect native protein in any of the tested *D. repens* lysates (female adult worm, adult worm E/S, microfilariae), indicating potential specificity of the antigen for L3 larvae. In case of *B. malayi alt-1* expression is terminated abruptly just after injection into the mammalian host tissues, but *alt-2* expression is less rigorously controlled, and trace levels of the transcripts were observed in all life cycle stages. At the protein level, both variants of *B. malayi* ALTs are L3 specific, similar to its orthologs in *D. immitis* (Di20/22)^{11,15,16}. The antigens are stockpiled in the glandular esophagus in the form of inclusion bodies during larval growth in the mosquito and are later secreted via pseudocoelom and cuticle upon entry into the definitive host tissues, triggered by an increase in temperature^{11,12}.

Furthermore, in immunohistochemistry, we observed a strong immunolabeling across almost the entire female cross-section, suggesting that the obtained anti-Dr20/22 serum may react non-specifically with other *D. repens* antigens, similar to what has been reported in the case of *O. volvulus*^{12,27}. Although we were unable to directly compare the Dr20/22 expression level to L3 larvae due to the unavailability of L3 samples, our findings, in combination with available literature, lead us to propose that Dr20/22, like its orthologues, is specific to the infective larvae stage.

There are several potential explanations for why we were not able to detect the antigen in the studied stages. Firstly, it is possible that the expression level was too low to be detected using the described techniques. However, we reject this possibility, as in our previous study, we successfully identified Dre33 in microfilariae lysate, which

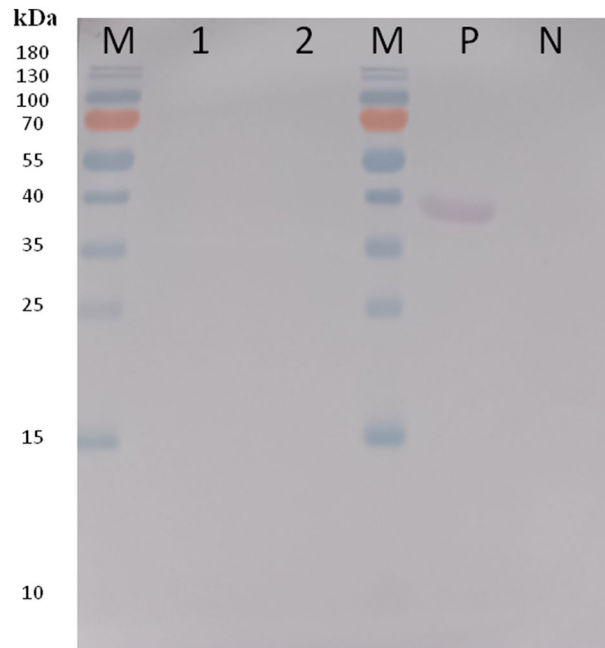


Figure 3. Staining of glycosylated proteins. The cropped blot is used in the figure. Lane M—weight marker (PageRuler Prestained Protein Ladder, 10 to 180 kDa, Thermo Scientific); lane 1—5 μ g of the rDr20/22; lane 2—10 μ g of the rDr20/22; P—positive control (horseradish peroxidase); N—negative control (soybean trypsin inhibitor). Both positive and negative controls were provided by the manufacturer. Original blot is presented in Supplementary Fig. 3.

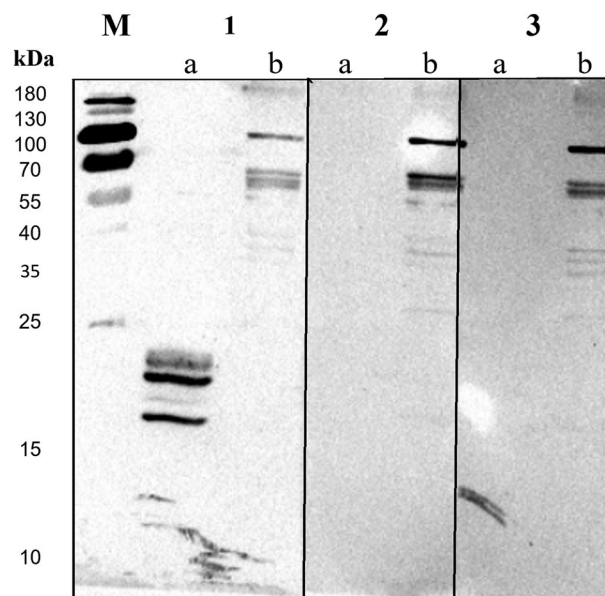


Figure 4. Western blot analysis of the specificity of anti-Dr20/22 antibodies to recombinant Dr20/22 (a) and native protein (b) in adult *D. repens* homogenate using mouse anti-Dr20/22 serum (1), and sera from non-immunized mice (2 and 3). The cropped blot is used in the figure. The nitrocellulose membrane was cut after an electrotransfer of the polyacrylamide gel. Lane M—molecular weight marker (PageRuler Prestained Protein Ladder, 10 to 180 kDa, Thermo Scientific). Original blot is presented in Supplementary Fig. 3.

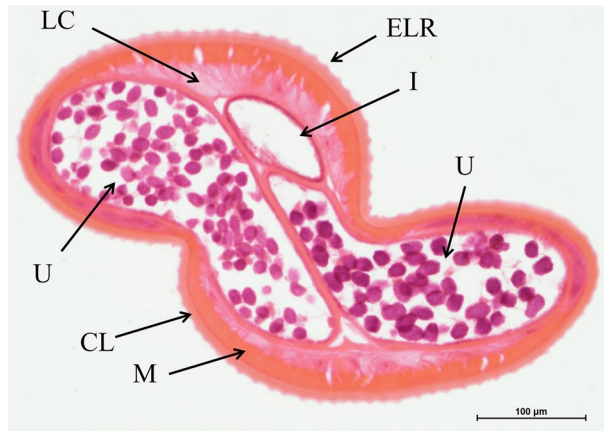


Figure 5. Morphological details of a *D. repens* female transverse section stained with H&E. *ELR* external longitudinal ridges, *CL* cuticular layer, *LC* lateral chord, *M* longitudinal muscles, *I* intestine, *U* uterus containing microfilariae.

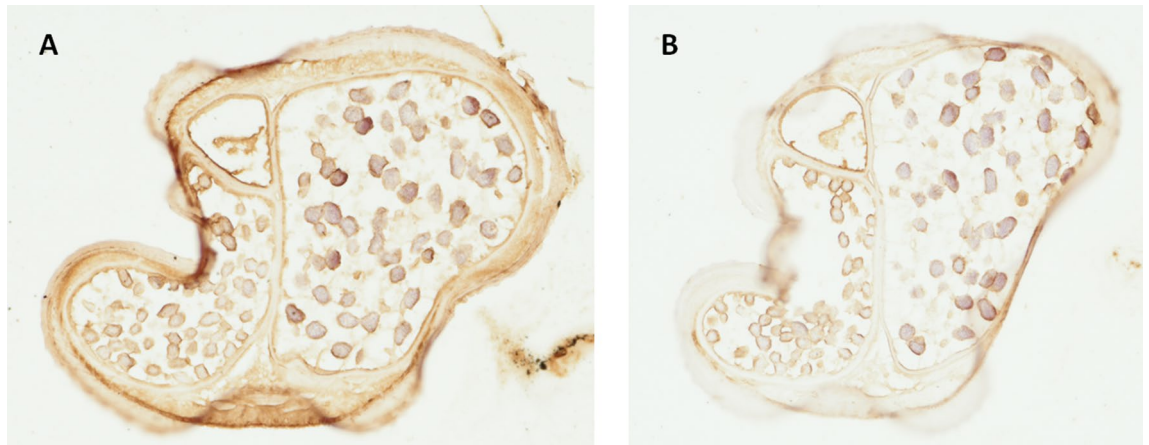


Figure 6. Immunohistochemistry staining of a *D. repens* female transverse sections with anti-Dr20/22 serum (A) and non-immunized mouse serum (B).

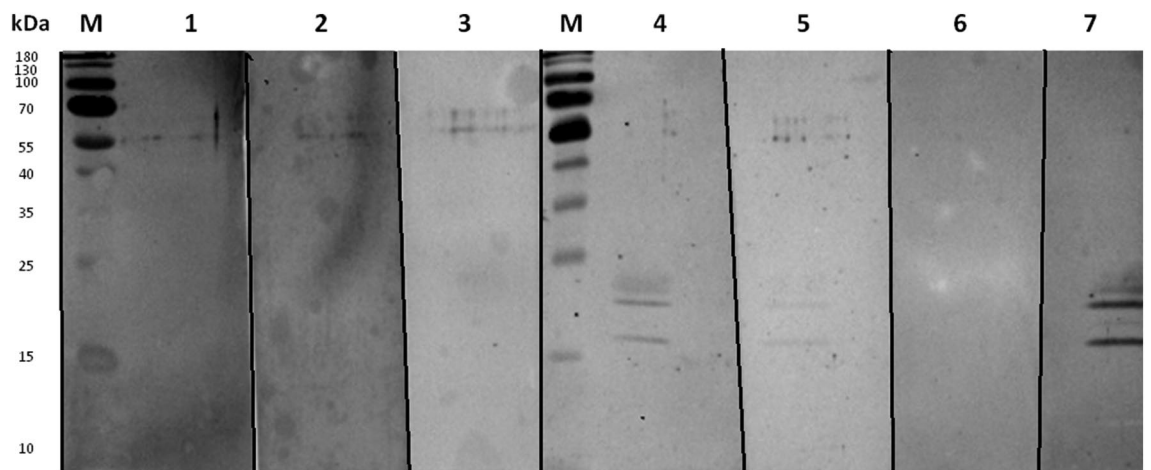


Figure 7. Western blot analysis of the presence of IgG specific to rDr20/22 in sera from dogs infected with *D. immitis* (1–3), *D. repens* (4, 5, 7) and negative dog (6). The cropped blot is used in the figure. The nitrocellulose membrane was cut after an electrotransfer of the polyacrylamide gel. Lane M—molecular weight marker (PageRuler Prestained Protein Ladder, 10 to 180 kDa, Thermo Scientific). Original blots are presented in Supplementary Fig. 3.

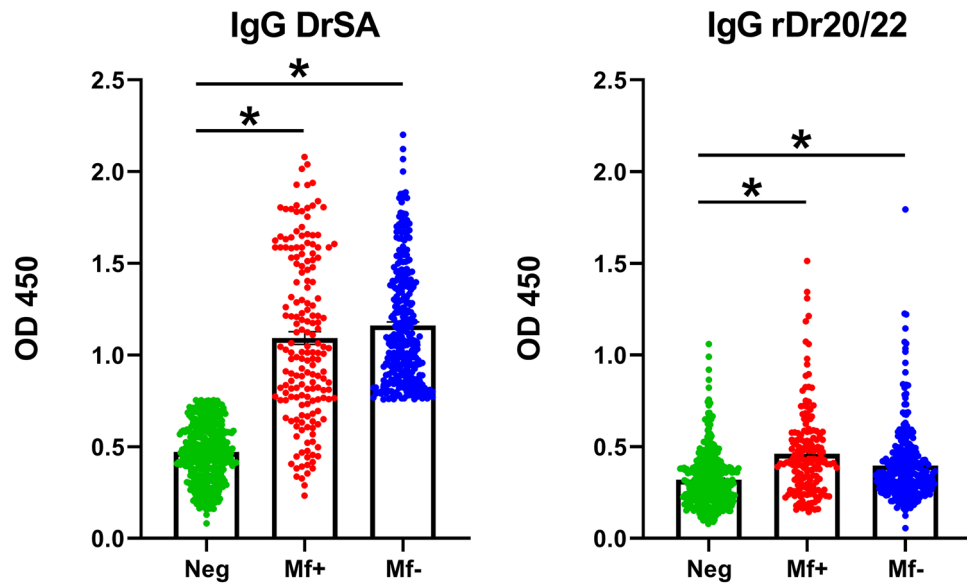


Figure 8. Diagnostic efficiency of rDr20/22 was assessed based on sera from dogs classified using *D. repens* somatic antigen (DrSA) ELISA: microfilaremic (Mf+; N = 174), amicrofilaremic (Mf-; N = 297) and negative (Neg; N = 379). The IgG response to rDr20/22 was demonstrated in both infected (Mf+, Mf-) and uninfected dogs. The statistically significant differences between examined groups are marked with an asterisk: * $p < 0.05$.

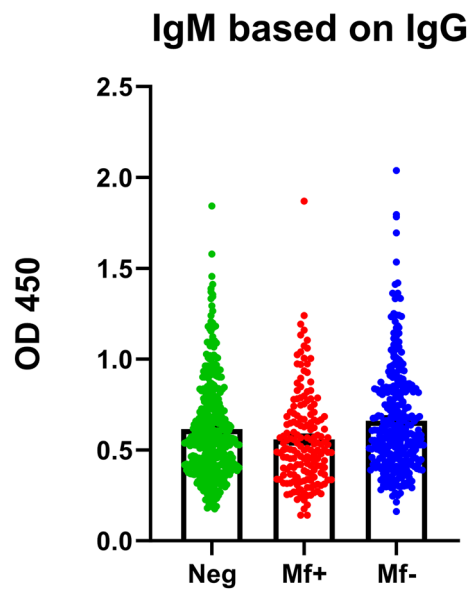


Figure 9. *D. repens* somatic antigen (DrSA) ELISA did not show statistically significant differences in IgM level between infected and non-infected groups. The IgM response to crude antigen from adult worms (DrSA) was evaluated in groups of dogs classified based on IgG level: microfilaremic (red; N = 174); amicrofilaremic (blue; N = 297), negative (green; N = 379).

presented a similar mRNA expression level to Dr20/22²⁸. The second, more plausible scenario involves molecular mechanisms responsible for the regulation of gene expression during larvae development. This phenomenon has been observed in research on *A. viteae* ES-62 antigen, where despite mRNA being expressed across the worm's life cycle, the protein is only secreted by L4 and adult worms and has never been detected in the filarial stages. The authors considered the possibility of different mRNA stability, but they ruled it out as the 3' UTRs were found to be identical in all stages²⁹. Additionally, various regulatory elements, both constructed and unconstructed (linear), play a leading role in translation and are located in the 5' UTR³⁰.

One such regulatory element is the spliced leader (SL) sequence, a short RNA containing a hypermodified 5'-cap structure that is transcribed from a different genomic location and transferred to the 5' end of designated

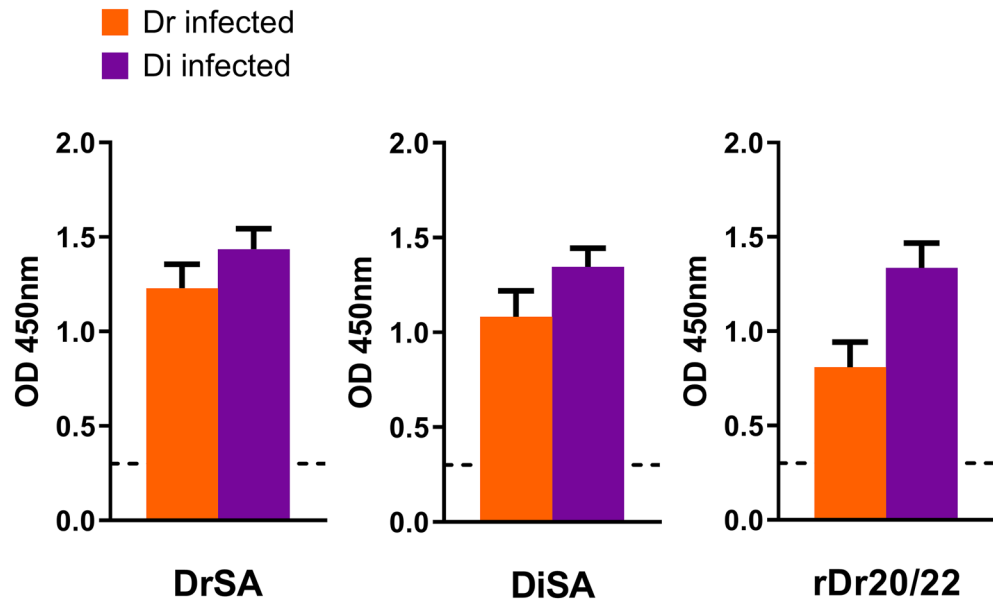


Figure 10. ELISA with crude antigen from adult worms of both species (DrSA/DiSA), as well as rDr20/22, showed cross-reactivity of IgG from dogs infected with either *D. repens* (red; N = 9) or *D. immitis* (blue; N = 9). The dashed line indicates uninfected (negative) dogs (N = 3–5).

mRNAs in a process known as spliced leader trans-splicing (SLTS)³¹. SLTS was first described in 1982 in African trypanosomes in mRNAs encoding variant surface glycoproteins³². It has since been observed in several other phyla, including cestodes, trematodes, and nematodes^{33–35}. In nematodes like *Ascaris lumbricoides* and *Caenorhabditis elegans*, the overall frequency of trans-spliced mRNAs ranges from 50% to even 90% depending on the source^{36–39}. The exact mechanism of SLTS remains puzzling, but several distinct functions have been proposed, including providing a 5'-cap structure for protein-coding RNAs, resolving polycistronic into individual capped, monocistronic mRNAs, enhancing mRNA translational efficiency through the hypermodified cap structure and/or leader sequence, and trimming and sanitizing 5' UTRs of the pre-mRNAs³¹.

In most research on filarial ALTs, the antigens were cloned using an L3-derived RNA template and primers specific for the spliced leader (SL) sequence^{10,12,13}. However, in the present study, we did not detect the SL in *dr20/22* (*D. repens* homologue of *alt*) in any of the examined stages. Given the fact that we previously identified the same SL sequence (specific for all nematodes) in adult worm mRNA encoding the ES62 antigen, known to be an adult stage-specific antigen, we considered whether the SLTS in *D. repens* may be differentially regulated throughout the parasite's life cycle. Several studies suggest that leader sequence-containing transcripts may be stage-specific or developmentally regulated, which might account for differential protein levels and protein repertoires in different stages^{40–43}. As the parasite's development is usually related to changes in the host/habitat, the involvement of environmental and physiological factors in controlling translation via SLTS cannot be excluded. For example, it has been shown that heat shock can inhibit the SLTS process in selected genes of trypanosomes⁴⁴. In the study on the marine chordate *Oikopleura dioica*, it was observed that some of the SLs contain a TOP-like motif that may enable nutrient-dependent translation control of the trans-spliced mRNAs in response to changes in physiological and environmental conditions^{45,46}. Similar trans-spliced TOP mRNAs have also been presented in *C. elegans*, suggesting that this phenomenon may occur in other species as well⁴⁵.

Despite the enigmatic nature of the precise mechanism of SLTS, it has been demonstrated that the process impacts translation efficiency^{47–49}. For instance, a study on *A. lumbricoides* showed that the SL sequence and its hypermethylated cap enhance translational efficiency, especially at the initiation of protein synthesis³⁸. Furthermore, Lall et al.⁵⁰ suggested that both structures may impact translation initiation of the trans-spliced transcripts due to trimming of primary transcripts that are non-optimal for translation. Interestingly, in the study on trypanosomes, the authors suggested that omitting SLTS/polyadenylation sites during polycistronic RNA processing may lead to the generation of RNAs in a “translational latency state”, which can be stored for further processing into a mature transcript when required by the cell⁵¹.

To summarize, based on our findings and available data, we propose that *D. repens dr20/22* gene expression may be developmentally controlled by the SLTS. We hypothesize that in vertebrate-specific stages (mf, adult), the gene is transcribed into non-functional mRNAs, which contain problematic elements in the 5' UTR that prevent efficient translation. However, after the mosquito ingests microfilariae and the molting process starts, environmental or physiological changes promote SLTS events that sanitize *alt*'s 5' UTR and add a modified cap structure, resulting in effective translation. After injection of L3 into the definitive host tissues, the temperature seems to signal abrupt secretion of the antigen and SLTS inhibition at once, leading to the presence of only “latent” transcripts in the adult stage. For a better understanding of the gene expression pattern and detailed mechanism, further study should be conducted using *D. repens* L3 larvae.

Although ALT proteins were identified over 20 years ago, their biological activity and processes in which they are involved are still unknown. Some studies have reported a weak similarity to phospholipase A2 enzymes (PLA₂), which may be implicated in membrane homeostasis, remodeling, migration through host tissues, or signal transduction^{13,15}. In the present study, we excluded this hypothetical activity of Dr20/22 using a commercially available phospholipase A2 assay kit.

The second part of the study examined the diagnostic potential of the antigen. Despite its unknown biological function, the prophylactic potential of the antigen has been widely investigated, especially in human lymphatic filariasis caused by *B. malayi* and *W. bancrofti*^{11,14,17,18,20}. Given the apparent specificity of Dr20/22 for invasive larvae, similar to other ALT homologues, and fact that Western blot successfully detected rDr20/22-specific antibodies only in sera from dogs infected with *D. repens*, we opted to evaluate the antigen's diagnostic potential. We hypothesized that it may facilitate early diagnosis of dirofilariasis within a short period after infection. ELISA with Dr20/22 revealed the presence of specific IgG in both infected (Mf+, Mf-) and non-infected (negative) groups, similar to the findings in other filarial ALTs^{11,12,14,17,18}. Our findings subsequently unveiled a degree of cross-reactivity of the antigen with sera from both *D. repens* and *D. immitis*, thereby challenging its specificity and, by extension, its diagnostic value. A high genetic similarity between both species could explain the observed cross-reactions in both ELISA experiments with crude extracts and rDr20/22. Dr20/22 shares approximately 70% of sequence identity with its counterpart in *D. immitis* (Supplementary Fig. 2).

Interestingly, some research indicates that resistance to filarial diseases might be facilitated by antibodies that target ALT proteins^{16,52}. Studies have demonstrated a significant reduction in the sera's capacity from individuals living in endemic areas (referred to as endemic normals EN) to contribute to the elimination of *B. malayi* L3 larvae in ADCC assay when ALT-specific antibodies are removed⁵². This underscores the potential role of ALT-specific antibodies in mediating resistance to filarial infections. Given that ALT proteins are abundantly expressed in invasive larvae and lack mammalian homologues, they emerge as particularly promising candidates for vaccine development against filarial diseases. Depending on the study and adopted vaccine strategy (single molecule vs. cocktail of molecules), the protection efficacy ranges from 30 to 96% and 70% to 80% using only *alt* DNA and *alt* DNA mixed with other constructs, respectively^{21–24}. In the case of protein-based vaccines, the mean reduction of the alive larval burden reached 69% to 76% when using *B. malayi* ALTs^{11,21–23}, and 49.82% to 62.26% based on *W. bancrofti* recombinant ALT or ALT mutants (e.g. protein without acidic domain or signal peptide)¹⁴. These antigens provided better protection than any other previously tested filarial protein and reached efficacy that rivals vaccination with radiation-attenuated larvae⁵³.

In conclusion, our study provides valuable insights into the expression pattern and potential specificity of Dr20/22 in *D. repens*. It also highlights the role of SLTS in gene expression regulation during the parasite's life cycle. However, further research with L3 larvae is needed for a better understanding of the gene expression pattern and its mechanisms. Additionally, the biological activity and processes involving ALT proteins remain unknown, and more studies are required to explore their potential role in vaccination and immunity against filarial infections.

Materials and methods

Dr20/22 cloning and recombinant protein production

Total RNA was extracted from adult *D. repens* worms and microfilariae using the Total RNA Mini Kit (A&A Biotechnology), following the manufacturer's protocol. The adult worms were manually homogenized in phenol solution, while the microfilariae were isolated from blood using 5 µm filters (Whatman), suspended in phenol solution, and homogenized in TissueLyser LT (QIAGEN, Hilden, NRW, Germany). Each RNA sample (1 µg) was subjected to DNase treatment and cDNA synthesis using the RevertAid First Strand cDNA Synthesis Kit (Thermo Fisher Scientific) as per the manufacturer's instructions, with the PTX primer (5' GAA CTA GTC TCG AGT TTTTTTTTTTTTTTTTTT 3') replacing oligo (dT)₁₈. The adult worm cDNA mixture was used as a template in PCR with PTX and gene-specific ForDr20/22 (5' ATG AAC AAA CTT YTM ATA RTY YTY GGC 3') primers to amplify the sequence encoding the *D. repens* homologue of the ALT (Dr20/22). The gene-specific primer was designed based on homologous genes from closely related filariae species (GenBank: U29459.1, U47545.2, AF285860.1). The PCR reaction was performed under the following conditions: 3 min at 95 °C, 35 cycles of 95 °C for 30 s, 53 °C for 45 s, and 72 °C for 30 s, with a final extension step of 10 min at 72 °C. The full-length cDNA was ligated into the pGEM T-Easy vector (Promega) and sequenced using Sanger's method to confirm the specificity of the product. Additionally, PCR was performed with ForDrSL (5' GTT TTA ATT ACC CAA GTT TGA GG 3') and gene-specific RevDr20/22cnds (5' ATC ATA TGA GCA CTG CCA GTC 3') primers to test if the mature adult and microfilariae mRNAs are enriched with the spliced leader (SL) sequence specific for *D. repens*, as detected in a previous study (GenBank: MT071086.1). The reaction conditions were the same as described above.

Subsequently, cDNA encoding the mature protein (without the signal peptide) was amplified using gene-specific primers incorporating restriction enzyme sites and subcloned into the pPICZα A vector (Invitrogen) using *EcoRI* and *XbaI* enzymes and T4 ligase (Thermo Fisher Scientific). The resulting construct (10 µg) was linearized with *SacI* enzyme and used for electrotransformation of the *P. pastoris* X33 strain. Transfected cells were spread on YPDS plates with increasing concentrations of zeocin (100, 500, 1000 µg/ml) to select multi-copy recombinants. A single colony positive in PCR with 5AOX1 (5' GAC TGG TTC CAA TTG ACA AGC 3') and 3AOX1 (5' GCA AAT GGC ATT CTG ACA TCC 3') primers was used for expression in BMMY medium containing 0.5% methanol at 29.8 °C for 72 h. All yeast transformation, culture, transformant analysis, and protein expression procedures were performed according to the EasySelect Pichia Expression Kit (Invitrogen) protocols.

The protein was purified under native conditions using the Protino Ni-NTA Agarose for His-tag protein purification Kit (MACHEREY-NAGEL) with the gravity flow method, following the manufacturer's protocol.

Eluted fractions were concentrated and dialyzed against PBS using Amicon Ultra-15 Centrifugal Filter Units with a 3 kDa MWCO (Merck Millipore). Endotoxins were removed using High Capacity Endotoxin Removal Spin Columns (Pierce), and the purified rDr20/22 protein was filtered through 0.22 µm syringe filters (Millex, Merck Millipore). The protein concentration was determined using the BCA Protein Kit Assay (Pierce). The presence of purified Dr20/22 was confirmed by SDS-PAGE and Western blotting using the Anti-polyHistidine Peroxidase antibody (Merck Millipore). The occurrence of potential glycosylation sites was assessed using the Glycoprotein Staining Kit (Pierce).

Cloning of Dr20/22 gDNA

Adult *D. repens* worms were manually homogenized in Tris buffer, and genomic DNA (gDNA) was isolated using the Genomic Mini Kit (A&A Biotechnology) following the manufacturer's protocol. The isolated gDNA was utilized as a template in PCR with primers designed to target the start (ForDr20/22cnds 5' ATG AAC AAA CTT TTC ATA GTT CTT GGC 3') and stop (RevDr20/22cnds 5' ATC ATA TGA GCA CTG CCA GTC 3') codons of the coding sequence. This PCR amplification aimed to capture the full-length gene, including both exons and introns. The reaction conditions involved an initial denaturation at 95 °C for 3 min, followed by 35 cycles of denaturation at 95 °C for 30 s, annealing at 52 °C for 45 s, and extension at 72 °C for 2 min, with a final extension step of 10 min at 72 °C. The amplified product was then cloned into the pGEM T-Easy Vector (Promega) and subjected to Sanger sequencing. The obtained sequence data were subsequently used for the prediction of the gene structure, including the determination of the number of exons and introns.

Analysis of gene expression level

Gene expression levels were assessed using Real-Time PCR. Total RNA isolation, DNase treatment, and cDNA synthesis were performed following the previously described methods. PCR reactions were conducted in triplicates, employing a two-step fast cycle protocol with PowerUp SYBR Green Master Mix from Applied Biosystems. The melt curve step was carried out in a QuantStudio 6 Real-Time PCR system (Applied Biosystems). The PCR process involved UDG (Uracil-DNA Glycosylase) activation for 2 min at 50 °C, followed by initial denaturation for 2 min at 95 °C. Subsequently, 40 amplification cycles were executed, comprising 3 s at 95 °C and 30 s at 60 °C. The reaction mixture included 10 ng of cDNA from each life cycle stage (adult *D. repens* worm and microfilariae), 5 µl of PowerUp SYBR Green Master Mix (2X), forward (ForDr20/22RT 5' CAG CGA CGA AAG TTA TGC AGA AGA C 3') and reverse (RevDr20/22RT 5' AAT ATG CAC CAC GAT TGC GGT TCA C 3') primers at a final concentration of 0.6 µM, and sterile water to reach a final volume of 10 µl. The absolute copy number of the *dr20/22* gene was determined based on a standard curve ranging from one billion to ten copies per reaction, utilizing the data collected during the anneal/extension step.

Statistically significant differences between different life cycle stages were analyzed using the Student's *t*-test.

Bioinformatics analysis and structural prediction of *D. repens* Dr20/22 protein

Comparison of the nucleotide sequences of *alt* from closely related filariae in the GenBank database was performed using the Basic Local Alignment Search Tool (Blast) available at <http://www.ncbi.nlm.nih.gov/blast/Blast.cgi>. The amino acid sequence was obtained using the Translate tool available at <http://web.expasy.org/translate/>. Nucleotide and amino acid alignments, incorporating the novel *D. repens* Dr20/22 sequence and homologous sequences from related filariae, were constructed using Multalin accessible at <http://multalin.toulouse.inra.fr/multalin/>. The theoretical molecular weight and isoelectric point were estimated using the Compute pI/Mw tool (https://web.expasy.org/compute_pi/). The signal peptide was determined using the SignalP 5.0 server available at <https://services.healthtech.dtu.dk/services/SignalP-5.0/>. For the determination of N-glycosylation, O-glycosylation, and phosphorylation sites, NetOGlyc, NetNGlyc, and NetPhos, respectively, were employed and accessed at <https://www.cbs.dtu.dk/services>. The identification of characteristic domains was carried out using the InterProScan Sequence Search available at <https://www.ebi.ac.uk/interpro/>. Lastly, the probable three-dimensional structure of *D. repens* Dr20/22 was obtained and visualized using Phyre², accessible at <http://www.sbg.bio.ic.ac.uk/phyre2/>.

Dirofilaria E/S collection and tissue lysates preparation

Briefly, to collect *D. repens* excretory/secretory (E/S) products, several live worms obtained during surgical procedures were washed in PBS and then incubated in RPMI 1640 supplemented with penicillin (100 U/ml) and streptomycin (100 µg/ml) at 37 °C for 16 h. Fresh medium was replaced every 2 h, and the collected medium was stored at –70 °C until further analyses. Subsequently, the collected medium was centrifuged (8000×g, 10 min, 4 °C), concentrated, and dialyzed against cold sterile PBS using an Amicon Ultra-15 Centrifugal Filter Unit with a 3 kDa MWCO (Merck Millipore). The resulting product was then passed through a 0.22 µm filter.

For adult worm (*D. repens* and *D. immitis*) and microfilariae lysates, the procedures described in our previous studies were followed^{28,54}. Protein concentration in the lysates was determined by BCA assay (Pierce).

Preparation of mouse anti-Dr20/22 serum and western blotting analysis of *D. repens* proteins

Antiserum against recombinant Dr20/22 was generated through subcutaneous immunization of a BALB/c mouse with 100 µg of the recombinant protein, followed by three booster doses of 75, 50, and 25 µg on days 14, 28, and 42, respectively. Each dose was mixed with Imject Alum Adjuvant (Thermo Fisher Scientific) in a 1:3 ratio. On day 49, the mouse was euthanized, and blood was collected in tubes, incubated for 2 h at 37 °C, followed by overnight incubation at 4 °C. The next day, the blood was centrifuged for 10 min at 500×g, and the serum was stored at –70 °C until further analyses. All experiments were conducted following relevant guidelines and regulations, and ethical approval was obtained from the 2nd Local Ethics Committee for Animal Experimentation,

Warsaw University of Life Sciences-SGGW, Poland (approval number: WAW2/82/2019). The manuscript reporting adheres to the recommendations in the ARRIVE guidelines⁵⁵.

To determine the presence of antibodies recognizing recombinant Dr20/22 epitopes in the mouse serum and to detect native protein in adult worm lysate, excretory/secretory (ES) products, and microfilariae lysate, Western blot analysis was performed. 0.25 µg of the recombinant protein and 10 µg of each lysate were separated on a 15% polyacrylamide gel during SDS-PAGE and subsequently transferred to a nitrocellulose membrane. The membrane was blocked for 2 h at room temperature using SuperBlock T20 (Thermo Fisher Scientific) and then incubated overnight at 4 °C with mouse anti-Dr20/22 serum or serum from non-immunized mice, both diluted 1:1000 in the blocking buffer. The following day, the membrane was thoroughly washed with PBS containing 0.05% Tween-20 (0.05% PBS-T) and then incubated for 1 h at room temperature with Anti-Mouse IgG HRP-conjugated antibodies (R&D Systems), diluted 1:1000 in the blocking buffer. After washing with 0.05% PBS-T (3 × 10 min), the membrane was visualized by chemiluminescence using SuperSignal West Pico PLUS Chemiluminescent Substrate (Thermo Fisher Scientific) in a ChemiDoc MP Imaging System (Bio-Rad).

Immunohistochemical detection of Dr20/22 protein in adult female *D. repens* worm

Detection of the Dr20/22 protein in adult female *D. repens* worms was carried out using immunohistochemistry staining. The worms were fixed in 4% buffered formalin, embedded in paraffin, and cross-sectioned to a thickness of 5 µm using a Leica RM2025 microtome (Leica Microsystems, Germany). The obtained histological sections were initially subjected to topographic staining using the hematoxylin–eosin (H/E) standard protocol to assess the morphology of the adult nematode.

For the immunohistochemistry staining, the histological slides were deparaffinized in xylene, rehydrated through a gradient of ethanol (from absolute alcohol to 70%), and then subjected to antigen retrieval by incubation for 5 min at 82 °C in 10 mM citric acid (pH 6). Endogenous peroxidase was blocked using 5% hydrogen peroxide, and to reduce non-specific antibody binding, the slides were blocked with Protein Blocker (Novocastra Peroxidase Detection System, Leica) and 5% skim milk, each step lasting 30 min at 37 °C. Subsequently, the slides were incubated with polyclonal anti-Dr20/22 mouse serum, diluted 1:100 in PBS, overnight at 4 °C. The following day, incubation with secondary antibodies and visualization were performed according to the manufacturer's protocol (Novocastra Peroxidase Detection System, Leica). After each step, the slides were rinsed in Tris buffer (pH 8.0, Merck Millipore). Finally, the slides were counterstained with Harris hematoxylin solution, differentiated with 1% acid alcohol, dehydrated, rinsed in xylene, and mounted in DPX Mountant for histology (Merck Millipore). For the negative control test, sera from non-immunized mice were used.

Immunological analysis of Dr20/22 antibodies in dogs infected with *D. repens* or *D. immitis*

Western blot analysis was performed to determine the presence of antibodies specific for rDr20/22 in sera from dogs infected with *D. repens* or *D. immitis*. The membrane was incubated with sera from infected or healthy (uninfected) dogs, diluted 1:400 in the blocking buffer, overnight at 4 °C. Subsequently, secondary anti-dog IgG-HRP antibodies (Abcam) were incubated for 1 h at room temperature in a 1:25,000 dilution. The remaining procedure steps, including protein separation on the gel, washing, and visualization, were conducted as described in section “Preparation of mouse anti-Dr20/22 serum and western blotting analysis of *D. repens* proteins”.

Overview of study design and diagnostic evaluation

The aim of our study was to compare the diagnostic efficiency of rDr20/22 to DrSA ELISA. We analyzed sera from 850 dogs, comprising 174 with active microfilaremia and 676 individuals without active microfilaremia—negative in PCR or Knott's test. Considering the possibility of occult/amicrofilaremic infections, we categorized the dogs using DrSA ELISA into three groups: microfilaremic (Mf+), amicrofilaremic (Mf-), and negative (Neg), based on the calculated cut-off value, which was determined as the mean OD plus 3 standard deviations (SD) from 35 dogs known to be negative in Knott, qPCR, and ELISA, as detailed in our previous study⁵⁴. Additionally, we examined the IgM response among each group and the IgG response against rDr20/22 using the same panel of sera.

Recognizing the high genetic similarity between *D. repens* and *D. immitis*, we conducted separate experiments to explore the potential occurrence of cross-reactions between both species. This investigation included the use of ELISA with extracts of adult worms (DrSA/DiSA) as well as rDr20/22. For these experiments, we utilized smaller groups of dogs, consisting of those infected with *D. repens* (N = 9), *D. immitis* (N = 9), and negative (N = 3–5).

Comparative diagnostic evaluation of rDr20/22 ELISA and crude adult worm antigens in canine dirofilariasis

The Nunc MaxiSorp C-shaped Plates (Thermo Fisher) were coated with 2.5 µg/ml of DrSA/DiSA in 0.1 M sodium carbonate buffer (pH 9.5) and incubated overnight at 4 °C. Subsequently, the plates were blocked with 0.1 M NaHCO₃ (pH 8.6) and 0.5% BSA for 1.5 h at room temperature. Plasma samples, collected during previous studies⁵⁴, were analyzed in a dilution of 1:1600 in the blocking buffer for 1.5 h at room temperature. The anti-dog peroxidase-conjugated IgG and IgM (Abcam) were diluted to 1:50,000 in 0.1 M NaHCO₃ (pH 8.6) and 0.5% BSA and then incubated for 1 h at room temperature. After each step, the plates were washed three times with PBS containing 0.05% Tween-20. TMB substrate solution was added to the wells, developed at room temperature, and the reaction was stopped after 30 min with 2 M H₂SO₄. Optical densities were measured at 450 nm using a microplate reader (Synergy HT, BioTek).

The ELISA with rDr20/22 was conducted similarly, all procedures were performed as described above, with the exception of the dogs' sera, which were used in a dilution of 1:400.

Evaluating the phospholipase A2 (PLA₂) activity of rDr20/22

The potential phospholipase A2 (PLA₂) activity of rDr20/22 was evaluated using the EnzChek Phospholipase A2 Assay Kit (Invitrogen). Fresh or frozen (stored at -80°C) protein was utilized in two-fold dilutions ranging from 100 μg per reaction to 0.2 μg per reaction. Additionally, the ability of rDr20/22 to inhibit PLA₂ activity was investigated. Each well was supplemented with 1.25 U/ml of PLA₂, which was pre-incubated for 20 min with serial dilutions of rDr20/22 (ranging from 100 to 0.2 μg per reaction) before the substrate-liposome mix was added. All reactions were conducted in a 96-Well Black Polystyrene Microplate (Costar) following the manufacturer's protocol.

The fluorescence was measured with excitation at $\sim 485/20$ nm and fluorescence emission at $\sim 528/20$ nm using a microplate reader (Synergy HT, BioTek). The PLA₂ activity was determined based on a standard curve ranging from 5 to 0.2 U/ml.

Statistical analysis

All data are presented as mean \pm standard error of the mean (SEM). Statistical analysis was performed using GraphPad Prism 8.0 (GraphPad Software, La Jolla, CA, USA) with unpaired *t*-test for gene expression analysis and Kruskal–Wallis test for data produced in ELISA. Differences between groups were considered statistically significant at $p < 0.05$.

Data availability

Sequence data that support the findings of this study have been deposited in the GenBank repository with the accession number MN706526.1. Other data is provided within the manuscript or supplementary information files.

Received: 20 November 2023; Accepted: 29 May 2024

Published online: 05 June 2024

References

- Fuehrer, H. P. *et al.* *Dirofilaria* spp. and *Angiostrongylus vasorum*: Current risk of spreading in central and northern Europe. *Pathogens* **10**, 1268. <https://doi.org/10.3390/pathogens10101268> (2021).
- Genchi, C. & Kramer, L. Subcutaneous dirofilariasis (*Dirofilaria repens*): An infection spreading throughout the old world. *Parasites Vectors* <https://doi.org/10.1186/s13071-017-2434-8> (2017).
- Baska, P. *et al.* *Fasciola hepatica*—The pilot study of *in vitro* assessing immune response against native and recombinant antigens of the fluke. *Acta Parasitol.* **58**, 453–462 (2013).
- Baska, P. & Norbury, L. J. The role of the intestinal epithelium in the ‘weep and sweep’ response during gastro-intestinal helminth infections. *Animals* **12**, 175 (2022).
- Zakeri, A., Hansen, E. P., Andersen, S. D., Williams, A. R. & Nejsum, P. Immunomodulation by helminths: Intracellular pathways and extracellular vesicles. *Front. Immunol.* **9**, 2349 (2018).
- Wiedemann, M. & Voehringer, D. Immunomodulation and immune escape strategies of gastrointestinal helminths and schistosomes. *Front. Immunol.* **11**, 572865 (2020).
- Bhoj, P., Togra, N., Khatri, V. & Goswami, K. Harnessing immune evasion strategy of lymphatic filariae: A therapeutic approach against inflammatory and infective pathology. *Vaccines* **10**, 1235 (2022).
- Devaney, E. & Osborne, J. The third-stage larva (L3) of *Brugia*: Its role in immune modulation and protective immunity. *Microbes Infect.* **2**, 1363–1371 (2000).
- Kwarteng, A. & Ahuno, S. T. Immunity in filarial infections: Lessons from animal models and human studies. *Scand. J. Immunol.* **85**, 251–257 (2017).
- Gregory, W. E., Blaxter, M. L. & Maizels, R. M. Differentially expressed, abundant trans-spliced cDNAs from larval *Brugia malayi*. *Mol. Biochem. Parasitol.* **87**, 85–95 (1997).
- Gregory, W. E., Atmadja, A. K., Allen, J. E. & Maizels, R. M. The abundant larval transcript-1 and -2 genes of *Brugia malayi* encode stage-specific candidate vaccine antigens for filariasis. *Infect. Immun.* **68**, 4174–4179 (2000).
- Wu, Y. *et al.* The Secreted Larval Acidic Proteins (SLAPs) of *Onchocerca* spp. are encoded by orthologues of the alt gene family of *Brugia malayi* and have host protective potential. *Mol. Biochem. Parasitol.* **134**, 213–224 (2004).
- Pogonka, T., Oberländer, U., Marti, T. & Lucius, R. *Acanthocheilonema viteae*: Characterization of a molt-associated excretory/secretory 18-kDa protein. *Exp. Parasitol.* **93**, 73–81 (1999).
- Aparna, R. *et al.* *Wuchereria bancrofti* 20/22 a homologue of abundant larval transcript L3 stage filarial antigen: Molecular and immunological characterization. *Parasite Immunol.* **36**, 475–484 (2014).
- Frank, G. R., Tripp, C. A. & Grieve, R. B. Molecular cloning of a developmentally regulated protein isolated from excretory-secretory products of larval *Dirofilaria immitis*. *Mol. Biochem. Parasitol.* **75**, 231–240 (1996).
- Frank, G. R. & Grieve, R. B. Purification and characterization of three larval excretory-secretory proteins of *Dirofilaria immitis*. *Mol. Biochem. Parasitol.* **75**, 221–229 (1996).
- Paul, R., Saha, G., Selvaraja, V. & Kaliraj, P. Cloning, expression and characterization of *Brugia malayi* abundant larval protein transcript-2 (BmALT-2) expressed in *Pichia pastoris*. *Prep. Biochem. Biotechnol.* **31**, 403–410 (2016).
- Madhumathi, J. *et al.* Crucial epitopes of *Wuchereria bancrofti* abundant larval transcript recognized in natural infection. *Eur. J. Clin. Microbiol. Infect. Dis.* **29**, 1481–1486 (2010).
- Yasin, N. *et al.* Design, expression, and evaluation of novel multiepitope chimeric antigen of *Wuchereria bancrofti* for the diagnosis of lymphatic filariasis—A structure-based strategy. *Int. Immunopharmacol.* **83**, 106431 (2020).
- Prado, I. C., Mendes, V. G., Souza, A. L. A., Dutra, R. F. & De-Simone, S. G. Electrochemical immunosensor for differential diagnostic of *Wuchereria bancrofti* using a synthetic peptide. *Biosens. Bioelectron.* **113**, 9–15 (2018).
- Ramachandran, S. *et al.* The larval specific lymphatic filarial ALT-2: Induction of protection using protein or DNA vaccination. *Microbiol. Immunol.* **48**, 945–955 (2004).
- Thirugnanam, S. *et al.* *Brugia malayi*: Comparison of protective immune responses induced by Bm-alt-2 DNA, recombinant Bm-ALT-2 protein and prime-boost vaccine regimens in a jird model. *Exp. Parasitol.* **116**, 483–491 (2007).
- Vanam, U. *et al.* Evaluation of immunoprophylactic efficacy of *Brugia malayi* transglutaminase (BmTGA) in single and multiple antigen vaccination with BmALT-2 and BmTPX for human lymphatic filariasis. *Am. J. Trop. Med. Hyg.* **80**, 319–324 (2009).
- Anand, S. B., Kodumudi, K. N., Reddy, M. V. & Kaliraj, P. A combination of two *Brugia malayi* filarial vaccine candidate antigens (BmALT-2 and BmVAH) enhances immune responses and protection in jirds. *J. Helminthol.* **85**, 442–452 (2011).

25. Yu, L.-R. & Veenstra, T. D. Characterization of phosphorylated proteins using mass spectrometry. *Curr. Protein Pept. Sci.* **22**, 148 (2021).
26. Gomez-Escobar, N. *et al.* Abundant larval transcript-1 and -2 genes from *Brugia malayi*: Diversity of genomic environments but conservation of 5' promoter sequences functional in *Caenorhabditis elegans*. *Mol. Biochem. Parasitol.* **125**, 59–71 (2002).
27. Joseph, G. T., Huima, T. & Lustigman, S. Characterization of an *Onchocerca volvulus* L3-specific larval antigen, Ov-ALT-1. *Mol. Biochem. Parasitol.* **96**, 177–183 (1998).
28. Zawistowska-Deniziak, A. *et al.* Immunoproteomic analysis of *Dirofilaria repens* microfilariae and adult parasite stages. *Pathogens* **10**, 1–18 (2021).
29. Stepek, G., Houston, K. M., Goodridge, H. S., Devaney, E. & Harnett, W. Stage-specific and species-specific differences in the production of the mRNA and protein for the filarial nematode secreted product, ES-62. *Parasitology* **128**, 91–98 (2004).
30. Leppek, K., Das, R. & Barna, M. Functional 5' UTR mRNA structures in eukaryotic translation regulation and how to find them. *Nat. Rev. Mol. Cell Biol.* **19**, 158–174 (2018).
31. Hastings, K. E. M. SL trans-splicing: Easy come or easy go? *Trends Genet.* **21**, 240–247 (2005).
32. van der Ploeg, L. H. T. *et al.* RNA splicing is required to make the messenger RNA for a variant surface antigen in trypanosomes. *Nucleic Acids Res.* **10**, 3591 (1982).
33. Brehm, K., Jensen, K. & Frosch, M. mRNA trans-splicing in the human parasitic cestode *Echinococcus multilocularis*. *J. Biol. Chem.* **275**, 38311–38318 (2000).
34. Brehm, K., Hubert, K., Scitutto, E., Garate, T. & Frosch, M. Characterization of a spliced leader gene and of trans-spliced mRNAs from *Taenia solium*. *Mol. Biochem. Parasitol.* **122**, 105–110 (2002).
35. Davis, R. E. *et al.* RNA trans-splicing in *Fasciola hepatica*. Identification of a spliced leader (SL) RNA and SL sequences on mRNAs. *J. Biol. Chem.* **269**, 20026–20030 (1994).
36. Nilsen, T. W. Trans-splicing of nematode premessenger RNA. *Annu. Rev. Microbiol.* **47**, 413–440 (1993).
37. Nilsen, T. W. Trans-splicing: An update. *Mol. Biochem. Parasitol.* **73**, 1–6 (1995).
38. Maroney, P. A., Denker, J. A., Darzynkiewicz, E., Laneve, R. & Nilsen, T. W. Most mRNAs in the nematode *Ascaris lumbricoides* are trans-spliced: A role for spliced leader addition in translational efficiency. *RNA* **1**, 714 (1995).
39. Blaxter, M. & Liu, L. Nematode spliced leaders—Ubiquity, evolution and utility. *Int. J. Parasitol.* **26**, 1025–1033 (1996).
40. Bitar, M., Boroni, M., Macedo, A. M., Machado, C. R. & Franco, G. R. The spliced leader trans-splicing mechanism in different organisms: Molecular details and possible biological roles. *Front. Genet.* **4**, 199 (2013).
41. Zeng, W., Alarcon, C. M. & Donelson, J. E. Many transcribed regions of the *Onchocerca volvulus* genome contain the spliced leader sequence of *Caenorhabditis elegans*. *Mol. Cell. Biol.* **10**, 2765–2773 (1990).
42. Nilsson, D. *et al.* Spliced leader trapping reveals widespread alternative splicing patterns in the highly dynamic transcriptome of *Trypanosoma brucei*. *PLoS Pathog.* **6**, 21–22 (2010).
43. Parsons, M., Nelson, R. G., Watkins, K. P. & Agabian, N. Trypanosome mRNAs share a common 5' spliced leader sequence. *Cell* **38**, 309–316 (1984).
44. Muhich, M. L. & Boothroyd, J. C. Synthesis of trypanosome hsp70 mRNA is resistant to disruption of trans-splicing by heat shock. *J. Biol. Chem.* **264**, 7107–7110 (1989).
45. Danks, G. B. *et al.* Trans-splicing and operons in metazoans: Translational control in maternally regulated development and recovery from growth arrest. *Mol. Biol. Evol.* **32**, 585–599 (2015).
46. Meyuhas, O. Synthesis of the translational apparatus is regulated at the translational level. *Eur. J. Biochem.* **267**, 6321–6330 (2000).
47. Wallace, A. *et al.* The nematode eukaryotic translation initiation factor 4E/G complex works with a trans-spliced leader stem-loop to enable efficient translation of trimethylguanosine-capped RNAs. *Mol. Cell. Biol.* **30**, 1958–1970 (2010).
48. Yang, Y. F. *et al.* Trans-splicing enhances translational efficiency in *C. elegans*. *Genome Res.* **27**, 1525–1535 (2017).
49. Bernard, F., Dargère, D., Rechavi, O. & Dupuy, D. Quantitative analysis of *C. elegans* transcripts by Nanopore direct-cDNA sequencing reveals terminal hairpins in non trans-spliced mRNAs. *Nat. Commun.* **14**, 1229 (2023).
50. Lall, S. *et al.* Contribution of trans-splicing, 5'-leader length, cap-poly(A) synergism, and initiation factors to nematode translation in an *Ascaris suum* embryo cell-free system. *J. Biol. Chem.* **279**, 45573–45585 (2004).
51. Jäger, A. V., De Gaudenzi, J. G., Cassola, A., D'Orso, I. & Frasch, A. C. mRNA maturation by two-step trans-splicing/polyadenylation processing in trypanosomes. *Proc. Natl. Acad. Sci. USA* **104**, 2035–2042 (2007).
52. Dakshinamoorthy, G., Samykutty, A. K., Munirathinam, G., Reddy, M. V. & Kalyanasundaram, R. Multivalent fusion protein vaccine for lymphatic filariasis. *Vaccine* **31**, 1616–1622 (2013).
53. Yates, J. A. & Higashi, G. I. *Brugia malayi*: Vaccination of jirds with 60cobalt-attenuated infective stage larvae protects against homologous challenge. *Am. J. Trop. Med. Hyg.* **34**, 1132–1137 (1985).
54. Pękacz, M. *et al.* Selection of new diagnostic markers for *Dirofilaria repens* infections with the use of phage display technology. *Sci. Rep.* **12**, 2288 (2022).
55. Kilkenny, C., Browne, W. J., Cuthi, I., Emerson, M. & Altman, D. G. Improving bioscience research reporting: The ARRIVE guidelines for reporting animal research. *Vet. Clin. Pathol.* **41**, 27–31 (2012).

Author contributions

Conceptualization, M.P., M.W. and A.Z.-D.; methodology, M.P., M.W., and A.Z.-D.; validation, M.P., K.B., M.K.; formal analysis, M.P., K.B.; investigation, M.P., K.B., M.K.; resources, M.P., E.C. and RM.; data curation, M.P.; writing—original draft preparation, M.P.; writing—review and editing, M.P., D.M., M.W. and A.Z.-D.; visualization, M.P. and A.Z.-D.; supervision, M.W. and A.Z.-D.; project administration, A.Z.-D.; All authors have read and agreed to the published version of the manuscript.

Funding

This research was funded by National Centre for Research and Development, grant number 0106/L-9/2017.

Competing interests

The authors declare no competing interests.

Additional information

Supplementary Information The online version contains supplementary material available at <https://doi.org/10.1038/s41598-024-63523-9>.

Correspondence and requests for materials should be addressed to A.Z.-D.

Reprints and permissions information is available at www.nature.com/reprints.

Publisher's note Springer Nature remains neutral with regard to jurisdictional claims in published maps and institutional affiliations.



Open Access This article is licensed under a Creative Commons Attribution 4.0 International License, which permits use, sharing, adaptation, distribution and reproduction in any medium or format, as long as you give appropriate credit to the original author(s) and the source, provide a link to the Creative Commons licence, and indicate if changes were made. The images or other third party material in this article are included in the article's Creative Commons licence, unless indicated otherwise in a credit line to the material. If material is not included in the article's Creative Commons licence and your intended use is not permitted by statutory regulation or exceeds the permitted use, you will need to obtain permission directly from the copyright holder. To view a copy of this licence, visit <http://creativecommons.org/licenses/by/4.0/>.

© The Author(s) 2024